ISSN 2089-8673 (Print) | ISSN 2548-4265 (Online)
Volume 13, Issue 2, July 2024

COMPARATIVE ANALYSIS OF CNN METHODS FOR PERIAPICAL RADIOGRAPH CLASSIFICATION

Made Windu Antara Kesiman[1], I Made Gede Sunarya[2],
I Gusti Lanang Trisna Sumantara[3]

[1,2,3]Pascasarjana Program Studi Ilmu Komputer, Universitas Pendidikan Ganesha

email: antara.kesiman@undiksha.ac.id[1], sunarya@undiksha.ac.id[2], lanang.trisna@undiksha.ac.id[3]

Abstract

Periapical radiographs are commonly used by dentists to diagnose dental problems and overall dental health conditions. The varying abilities of dentists to diagnose may be limited by their visual acuity and individual skills. To address this issue, there is a need for an application capable of computationally recognizing and classifying periapical radiographs. The commonly used computational method for image processing, specifically image recognition, is the Convolutional Neural Network (CNN) method. This study aims to create an application that can classify periapical radiographs and analyze the capabilities of the Convolutional Neural Network (CNN) method in this classification process. In general, periapical classification is divided into five types: Primary Endo with Secondary Perio, Primary Endodontic Lesion, Primary Perio with Secondary Endo, Primary Periodontal Lesion, and True Combined Lesions. The periapical radiograph classification process was tested using four CNN models: ResNet50v2, EfficientNetB1, MobileNet, and Shalow CNN. The evaluation of the CNN method utilized a confusion matrix-based technique to generate accuracy, precision, recall, F1-score and Weighted Average F1-score values. Based on the evaluation results, the highest accuracy value was achieved by EfficientNetB1 with 82%, followed by ResNet50v2 with 76%, MobileNet with 75%, and Shallow CNN with 71%.

Keywords: Periapical radiographs, Convolutional Neural Network (CNN), Primary Endodontic Lesion, F1-Score, Precision, EfficientNetB1, ResNet50v2, MobileNet.

Received: 11-12-2023 | **Revised:** 26-04-2024 | **Accepted:** 30-04-2024
DOI: https://doi.org/10.23887/janapati.v13i2.71664

INTRODUCTION

Teeth are an important organ found in the oral cavity. They serve various functions, such as speech, chewing food, and contributing to facial aesthetics, supporting one's appearance. Teeth are composed of several parts, namely enamel, dentin, pulp, and nerve tissue [1].

The pulp tissue and the surrounding tissues of the tooth (periodontal) have a close relationship. Abnormal conditions in these tissues are referred to as lesions. There are several lesions that can occur in the pulp and surrounding tissues of the tooth, namely endodontic lesions, periodontal lesions, and endoperio lesions. Endodontic lesions are generally caused by infections resulting from bacteria within the tooth's root canal. Periodontal lesions are inflammations or swellings caused by the accumulation of plaque and dental calculus (tartar). When both endodontic and periodontal lesions affect a single tooth simultaneously, they are referred to as endoperio lesions [2].

Periapical radiograph is a type of radiographic image taken inside the oral cavity, used to provide an overview of the entire tooth surface from the crown to the root, the supporting bone structure, and the surrounding tissues of the tooth [3]. Periapical radiography aims to obtain an overall view of the soft tissue surrounding the tooth, including from the crown to the tip of the tooth root (apical area). Periapical diseases can be caused by infections originating from the pulp tissue.

The results of periapical radiographs will be interpreted by the dentist to obtain a final diagnosis. The interpretation process may be limited by variations in visual acuity and individual skills among dentists. Therefore, a system is needed to diagnose and classify abnormalities from the obtained radiographic images.

In response to the issue of interpreting images and classifying abnormalities from the obtained periapical radiographs, an idea and concept emerged to perform computed analysis of periapical radiographic data.

The method used for this purpose is the Convolutional Neural Network (CNN) method. CNN is a method of artificial neural networks that utilizes several layers to perform learning, inspired by the neural network concept observed in mammals for visual perception. CNN's approach to image recognition involves learning patterns from an image based on training data, which serves as a model to produce optimal outputs for recognizing an image. [4].

The previous research used the CNN method to classify dental caries and infections with the title Classification of Dental Disease using CNN, achieving an accuracy result of 88.46% [5]. The research Automatic Lesion Detection in Periapical X-rays combines CNN with SVM and achieves an accuracy result of 98%[6].

In this research, classification experiments were exclusively conducted using the CNN method. Previous research experiments solely presented accuracy results, lacking detailed classification accuracy breakdowns to evaluate the strengths and weaknesses of the methods utilized in periapical classification. This research endeavors to offer deeper insights into the performance of the CNN method in classifying periapical X-ray images, aiming to pinpoint areas where this method may be less effective or require improvement.

This research aims to analyze the capabilities of CNN by implementing 4 different methods, namely ResNet50v2, EfficientNetB1, MobileNet, and Shallow, in classifying periapical radiographs. The evaluation is carried out using a confusion matrix to obtain the best F-1 score value.

These four models represent various approaches to CNN architecture, ranging from the deeper and more complex (ResNet50v2), to the more parameter-efficient and computationally efficient (EfficientNetB1), suitable for lighter devices (MobileNet) and the role model CNN architecture (Shallow CNN). By comparing the performance of these four models, the study can provide insights into the relative strengths and weaknesses of each method.

In this research, the imbalance of the original periapical dataset was respected and not specifically adjusted to balance. The focus of the research was on conducting diverse experiments to best results. Instead, a weighted approach, method Weighted Average F1-Score was utilized to determine the final outcome.

STUDY LITERATURE

A. Rontgent Periapical

The periapical radiograph is a type of X-ray taken inside the oral cavity that serves to visualize the entire tooth, from the crown to the root, as well as the supporting bone and the surrounding tissues of the tooth [3].

Figure 1. Rontgent Periapical

Figure 1 is one example of a periapical radiograph. The radiographs provide information that can assist doctors in interpreting symptoms around the teeth.

B. Classification of Periapical Lesions

Abnormalities or periapical lesions come in various forms. Generally, these abnormalities are most commonly divided into five categories based on pathology in 1972 [7].

Primary Endodontic Lesions disease starts from the crown and pulp tissue then progresses, resulting in radiolucency on the tooth root. It does not or has not yet affected the periodontal tissue.

Figure 2. Primary Endodontic Lesions

Figure 2 is example of periapical endodontic lesion is observed spreading from the crown of the tooth and damaging the tooth crown, but it has not yet caused an abscess or boil in the root area of the tooth.

Primary Periodontal Lesions usually caused by bacteria in the periodontal tissues. Generally, there are no abnormalities in the crown, but plaque and calculus or dental tartar are often found in these lesions.

ISSN 2089-8673 (Print) | ISSN 2548-4265 (Online)
Volume 13, Issue 2, July 2024

Figure 3. Primary Periodontal Lesions

Figure 3 there are no lesions or abnormalities present in the crown area, while inflammation is observed in the periodontal tissue.

Primary Endo with Secondary Perio disease originates from damage to the crown and pulp tissue, then spreads towards the periodontal tissue.

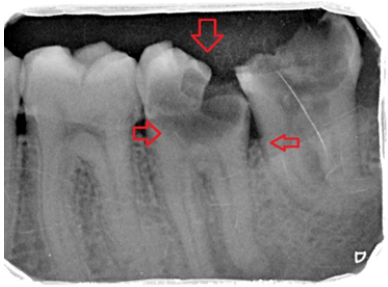

Figure 4. Primary Endo with Secondary Perio

Figure 4, the damage to the tooth is observed in both the crown and pulp, indicating its potential progression towards the periodontal tissue.

Primary Perio with Secondary Endo occurs due to inadequate management of the periodontal tissue, leading to its spread towards the tooth root, ultimately affecting the pulp tissue.

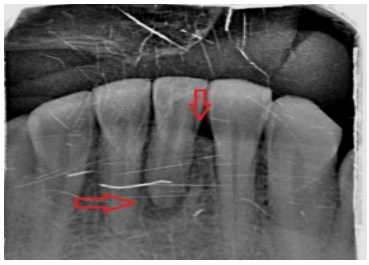

Figure 5. Primary Perio with Secondary Endo

Typically, there is no damage to the crown in this lesion as seen in Figure 5.

True Combined Lesions disease is caused by two concurrent conditions: periodontal disease and pulp disease. It is difficult to determine the origin from which the lesion initially develops when damage to both tissues is extensive.

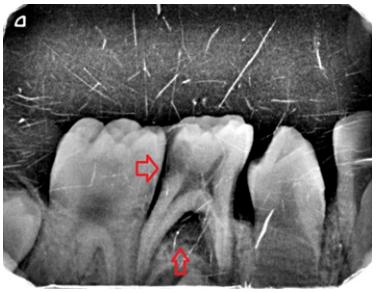

Figure 6. True Combined Lesions

Figure 6 shows a periodontal lesion or inflammation is observed in the area of the tissue that connects the teeth, along with inflammation in the pulp area.

C. Convolutional Neural Network (CNN)

The Convolutional Neural Network (CNN) is a part of deep neural networks that is commonly used for image data to perform detection and recognition of objects within an image [5]. Figure 7 represents an example of the basic CNN architecture.

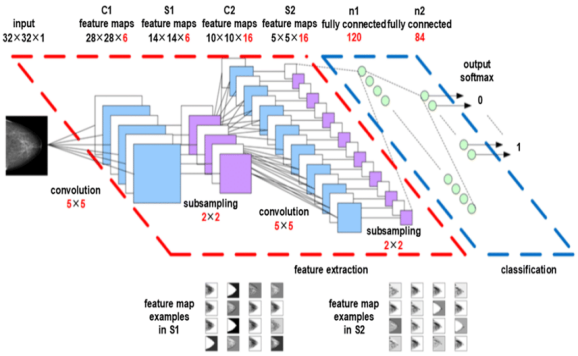

Figure 7. CNN Architecture

In its implementation, CNN has four main processes, namely the convolution layer, max pooling layer, fully connected layer, and activation layer.

D. ResNet50v2

ResNet-50v2 is one of the variants of the Convolutional Neural Network (CNN) architecture called ResNet (Residual Neural Network) version 2. ResNet-50v2 utilizes Residual Bottleneck blocks, where the blocks use bottleneck methods to reduce computational load. ResNet-50 v2 employs L2 Regularization technique to mitigate overfitting. Figure 8 displays the architecture of ResNet-50 v2.

ISSN 2089-8673 (Print) | ISSN 2548-4265 (Online)
Volume 13, Issue 2, July 2024

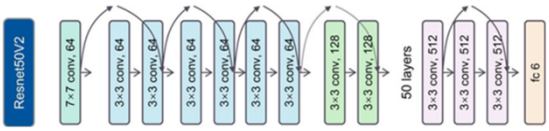

Figure 8. Resnet-50V2

E. EfficientNetB1

EfficientNet is a CNN model developed using a specialized transfer learning approach with the aim of recognizing and classifying images. The classification process is applied by considering the calculations of each layer, the channels used by the operators, and passing through multiple stages. [8].

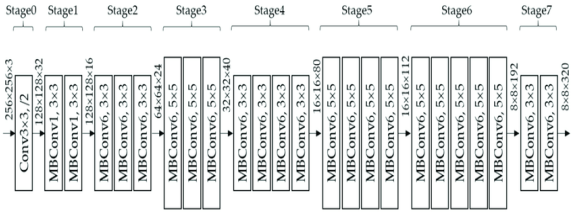

Figure 9. EfficientNetB1

Figure 9 displays the architecture of EfficientNetB1 with the resolution of channels and layers used in the convolution process.

F. MobileNet

MobileNet is a CNN method that implements efficiency in model deployment, usually used on mobile devices. It has a lightweight architecture capable of building a shallow network with low convolution process latency.

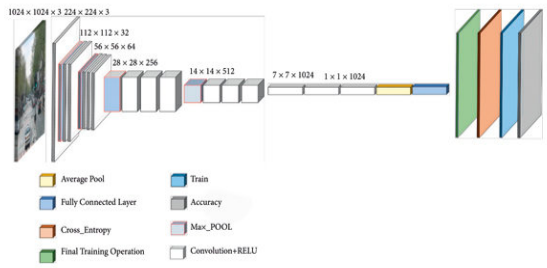

Figure 11. MobileNet

The basic architecture of MobileNet has a small structure and low latency; however, in many cases of usage or specific applications, a smaller and faster model is required. Figure 11 displays the type of convolution, the number of filter layers passed, and the input size of the convolution process.

G. Shallow CNN

Shallow CNN, short for Shallow Convolutional Neural Network, refers to a simplified architecture within the realm of artificial neural networks, specifically in the domain of image processing and pattern recognition. It represents a neural network structure that is comparatively simpler or less deep than more complex CNN architectures [9].

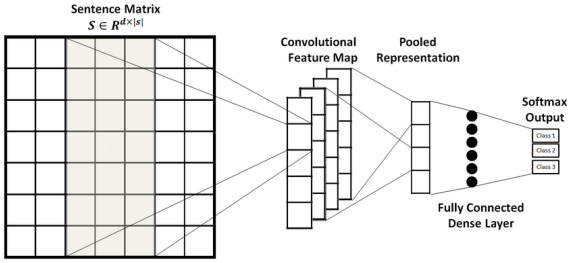

Figure 12. Shallow CNN

Architecture shallow CNN as seen in Figure 12 typically comprises fewer convolutional layers and pooling layers compared to deeper or more intricate CNN architectures like VGG, ResNet, or Inception. Despite its shallowness, these models can still be effective for specific tasks, particularly when dealing with less complex datasets or when computational resources are limited.

H. Confusion Matrix

The Confusion Matrix method is a measurement technique for classification that uses a confusion matrix table as seen in Table 1 to observe precision, recall, and F1-score values.

Table 1. Confusion Matrix

		Predicted Class	
		Positive	Negative
Actual Class	Positive	True Positive (TP)	False Negative (FN)
	Negative	False Positive (FP)	True Negative (TN)

P (Positive) represents the true positive outcome. N (Negative) represents the true negative outcomes. TP is the result of the system's positive prediction that matches the positive target. TN is the result of the system's negative prediction that matches the negative

target. FP is the result of the system's positive prediction, but the target outcome is negative. FN is the result of the system's negative prediction, but the target outcome is positive.

$$\text{Accuracy} = \frac{TP+FN}{P+N} \quad (1)$$

$$\text{Precision} = \frac{TP}{TP+FP} \quad (2)$$

$$\text{Recall} = \frac{TP}{TP+FN} \quad (3)$$

$$\text{F1-score} = 2x\frac{Precision\ x\ Recall}{Precison+Recall} \quad (4)$$

$$\text{Weighted Average F1-score} = \frac{\sum_i (F1_i \times Weight_i)}{\sum_i Weight_i)} \quad (5)$$

METHOD

The data used in this research consists of periapical X-ray data with 5 classifications. The research dataset was obtained from a collection of data gathered from the Armed Forces Dental Institute, Rawalpindi, Pakistan. The total number of images in the dataset is 534 and has been sorted by experienced radiologists and dentists. The five data sets are divided based on the dental disease lesions present in the periapical dental X-rays.

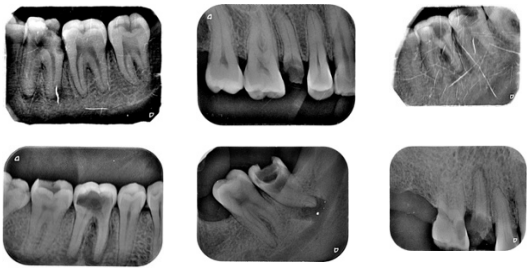

Figure 13. Dental X-ray Image Geometry

Periapical X-rays have different shapes depending on the position of the teeth in the mouth. Figure 13 shows samples of periapical X-rays with various shapes.

The periapical dataset is divided into 5 classifications with an 85:15 percentage split. This means 85% of the data is used for training, and 15% of the data is used for testing.

Table 2. Dataset Split

Periapical	Training	Test
Primary Endo with Secondary Perio	102	20
Primary Endodontic Lesion	108	16
Primary Perio with Secondary Endo	31	8
Primary Periodontal Lesion	101	17
True Combined Lesions	110	21

Table 2 shows the division of periapical data along with the number of data instances allocated to each category for training and testing.

Table 3. Hyperparameter Scenarios

Hyperparameter	Case
Epoch	25,40,75,100
Batch Size	8,16,32
Learning Rate	0.1, 0.01, 0.001, 0.0001

Testing will be conducted using hyperparameter scenarios to determine the best parameters for the CNN model. The hyperparameter testing for the Shallow CNN method will be applied to other CNN models as well. Table 3 displays the scenarios for testing hyperparameters in the CNN model. Three types of hyperparameters are modified to determine their optimal values.

Table 4. Augmented Image

Augmented	Size
Horizontal Flip	Auto
Vertical Flip	Auto
Rotate	20 °

The periapical radiographs dataset has imbalanced data, which requires additional data in the training set. In the case of the imbalanced periapical radiographs dataset, which requires additional data in the training set, the approach taken in this research was to respect the imbalance of the original dataset and not specifically adjust it to balance. Example, if 15% of images are augmented, then everything will be multiplied by 15%.

Table 4 shows the augmentation data applied during the testing process. Hyperparameters were selected based on the tooth geometry positions feasible for periapical radiographs.

ISSN 2089-8673 (Print) | ISSN 2548-4265 (Online)
Volume 13, Issue 2, July 2024

The CNN models built are ResNet50v2, EfficientNetB1, MobileNet, and Shallow CNN which were built and tested across several scenarios. The evaluation method is by comparing the test results based on the confusion matrix. The values of the confusion matrix will be used as references to determine the accuracy and F1-score of the CNN model testing using a weight-based approach.

RESULT AND DISCUSSION

The testing process begins with a manual search for optimal hyperparameter values. The testing is conducted using a shallow CNN model, which is built with a basic CNN architecture. In this process, CNN parameters are set manually. Each parameter has the ability to influence the model's performance during training and the output generated during the classification process.

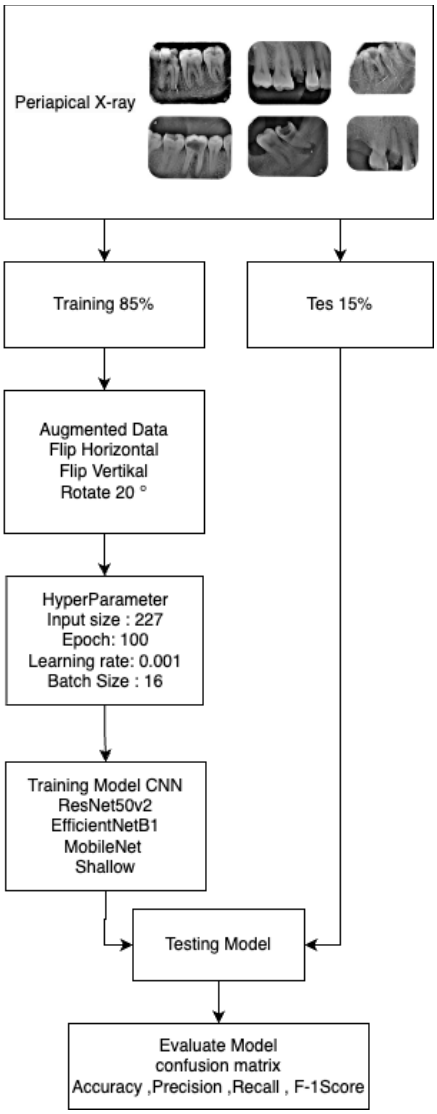

Figure 14. General Architecture

In general, the main steps of periapical X-ray classification can be observed in Figure 14. Figure 14 illustrates the classification process, commencing with the division of the dataset into training and test datasets. The subsequent step involves augmentation to increase the number of images in the training dataset, aligning with the characteristics of the X-ray data. Following this stage is the determination of hyperparameters for training.

The hyperparameters displayed in Figure 14 have been previously tested to identify their optimal values. Detailed information regarding these hyperparameter values is available in Table 5, 6, and 7.

Once everything is prepared, the training process is executed using 4 CNN models. The training results are then subjected to testing to evaluate the best achievable values by the trained models.

The selection of the best hyperparameters in this study was done by conducting several tests. The epochs were tested using batch sizes of 8, 16, and 32, with a learning rate of 0.001. The testing was conducted across 4 model epochs: 25, 50, 75, and 100 using the Shallow CNN method.

Table 5. Result Hyperparameter Epoch

Epoch	Batch Size	Learning Rate	Weight Average
25	8	0,001	0,41
50	8	0,001	0,63
75	8	0,001	0,68
100	8	0,001	0,70
25	16	0,001	0,42
50	16	0,001	0,66
75	16	0,001	0,67
100	16	0,001	0,71
25	32	0,001	0,40
50	32	0,001	0,44
75	32	0,001	0,70
100	32	0,001	0,70

Table 5 shows the highest F1-score with weight average was achieved at epoch 100 with a batch size of 16. Meanwhile, the lowest F1-score was observed at epoch 25 with a batch size of 32, recording a value of 0.40.

ISSN 2089-8673 (Print) | ISSN 2548-4265 (Online)
Volume 13, Issue 2, July 2024

Table 6. Result Batch Size

Batch Size	Accuracy
8	0,70
16	0,71
32	0,70

Based on the test results on Table 6, the highest accuracy was achieved with a batch size of 16, while batch sizes 8 and 32 exhibited the same level of accuracy.

Table 7. Result Learning Rate

Learning Rate	Accuracy
0.1	0.26
0.01	0.26
0.001	0.71
0.0001	0.59

Testing the hyperparameter learning rate shows that a learning rate of 0.001 achieves the best accuracy of 0.70.

Based on the testing of the three hyperparameters, the best values are selected based on the combination to be used as the reference hyperparameters in the main process, as seen in Figure 14.

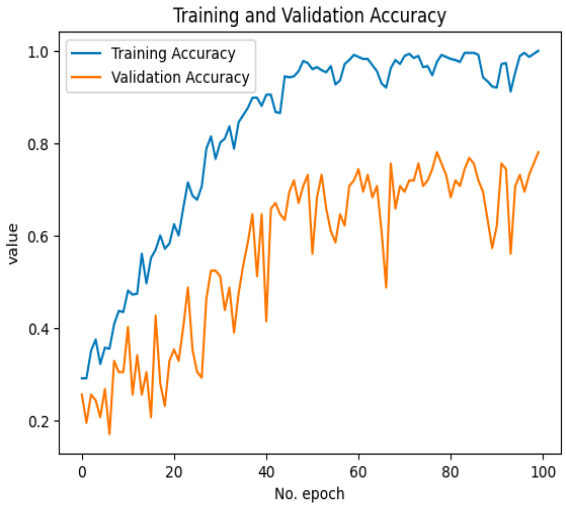

Figure 15. Accuracy Resnet50v2

Based on Figure 15, the performance of the ResNet50v2 model depicts a trend from the beginning to the end, showing that both training and validation accuracies experienced an increase. This indicates that the model was able to learn well, although the validation accuracy did not reach the same level as the training accuracy.

Figure 16. EfficientNetB1

EfficientNetB1, based on the training accuracy in Figure 16, exhibits high fluctuations in epochs 0-20, then fluctuations decrease and become more stable from epochs 20-100. The model's performance indicates good learning with not too high of an overfitting.

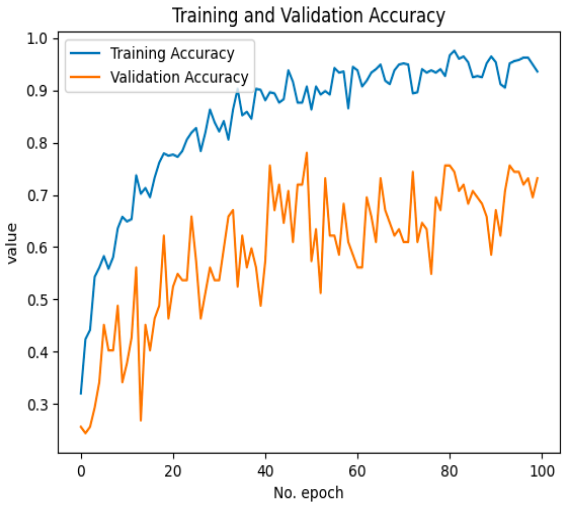

Figure 17. MobileNet

Based on Figure 17, the performance of the MobileNet model displays consistently high training accuracy, whereas the validation accuracy shows high fluctuations. The validation accuracy exhibits an upward trend from epoch 0 to 40 but then starts to plateau with a slight decline. This suggests that the MobileNet model experienced overfitting in the final epochs of learning.

ISSN 2089-8673 (Print) | ISSN 2548-4265 (Online)
Volume 13, Issue 2, July 2024

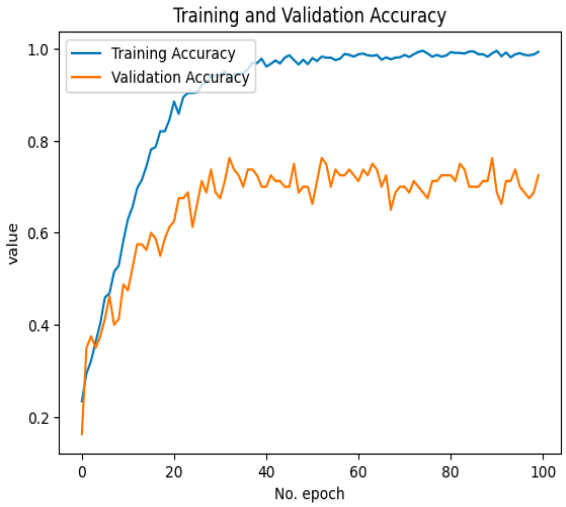

Figure 18. Shallow CNN

Figure 18 shows the performance of the Shallow CNN model. The training accuracy and validation accuracy appear to experience overfitting from epoch 40, tending to plateau and showing a slight decline. This indicates that the model struggled to learn from the trained dataset.

Table 8 shows that each model has its own level of confusion. This is influenced by the design of CNN and the depth of the network in the classification process of the model. Based on the confusion matrix, it can be observed that the models have confusion in classifying true combined lesions. This occurs because true combined lesions are a combination of endodontic lesions and periodontal lesions.

Table 8. Confusion Matrix

Resnet50v2	EfficinetNetb1
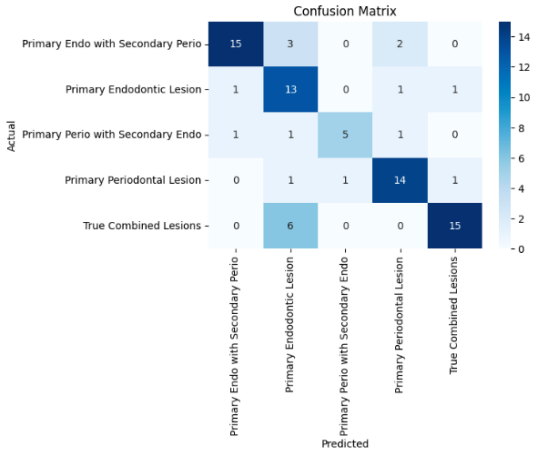	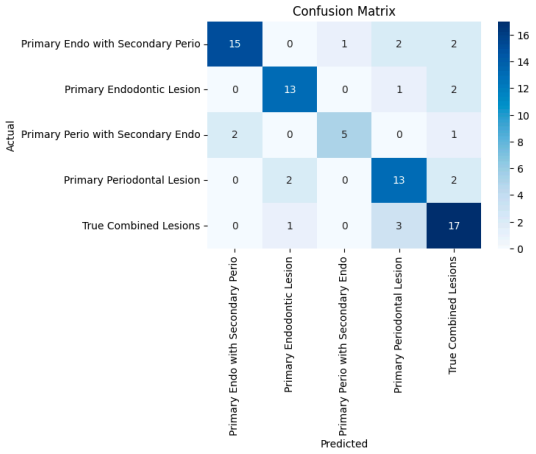
MobileNet	**Shallow**
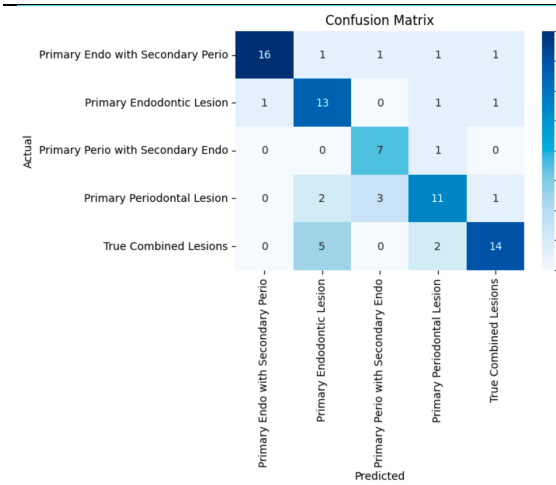	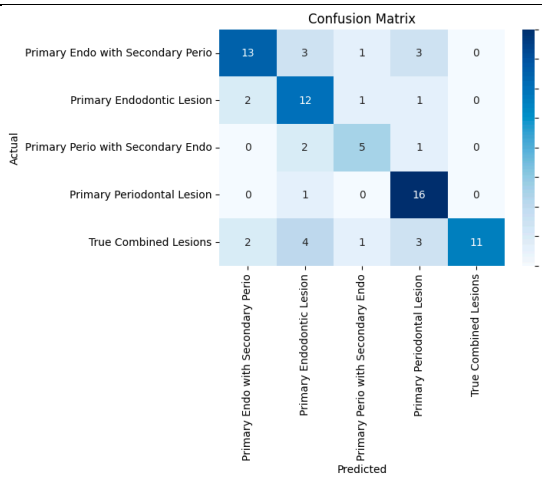

Table 9 demonstrates that the precision values for each classification data vary. EfficientNetB1 consistently shows the highest recall values across most periapical lesion types, indicating its strong ability to correctly classify positive cases of those lesions. It performs particularly well in Primary Perio with Secondary Endo and True Combined Lesions.

MobileNet also demonstrates good performance, especially in Primary Endo with Secondary Perio and Primary Periodontal Lesion.

ResNet50v2 performs well in classifying Primary Endo with Secondary Perio and True Combined Lesions, but it shows lower recall values in other lesion types compared to EfficientNetB1 and MobileNet.

The Shallow CNN model generally has lower recall values across all lesion types, indicating its limited capability compared to the other CNN models.

Overall, EfficientNetB1 exhibits the highest average recall (0.84), making it the most effective model in diagnosing periapical lesions in this study. MobileNet also performs well with an average recall of 0.77. The results indicate that the EfficientNetB1 and MobileNet models are more suitable for this classification task compared to ResNet50v2 and Shallow CNN models.

Table 9. CNN Model Precision Comparison

Periapical	ResNet50v2	EfficientNetB1	MobileNet	Shallow
Primary Endo with Secondary Perio	0,88	0,89	0,94	0,80
Primary Endodontic Lesion	0,76	0,76	0,62	0,46
Primary Perio with Secondary Endo	0,83	1	0,64	1,00
Primary Periodontal Lesion	0,68	0,65	0,69	0,78
True Combined Lesions	0,70	0,94	0,82	0,85
Weight Average F1-Score	0,76	0,84	0,77	0,76

Table 10 show EfficientNetB1 consistently shows the highest recall values across most periapical lesion types, indicating its strong ability to correctly classify positive cases of those lesions.

ResNet50v2 and EfficientNetB1 perform comparably well, with EfficientNetB1 having a slight advantage in recall values for Primary Endodontic Lesions and True Combined Lesions.

MobileNet performs well in classifying Primary Perio with Secondary Endo and Primary Periodontal Lesion cases, showing relatively high recall values.

The Shallow CNN model generally has the lowest recall values across all lesion types, indicating its limited capability compared to the other CNN models.

Overall, EfficientNetB1 exhibits the highest average recall (0.82), making it the most effective model in diagnosing periapical lesions in this study.

Table 10. Comparison Recall Model CNN

Periapical	ResNet50v2	EfficientNetB1	MobileNet	Shallow
Primary Endo with Secondary Perio	0,75	0,8	0,8	0,80
Primary Endodontic Lesion	0,81	0,81	0,81	0,75
Primary Perio with Secondary Endo	0,62	0,75	0,88	0,62
Primary Periodontal Lesion	0,76	0,88	0,65	0,82
True Combined Lesions	0,76	0,81	0,67	0,52
Weight Average F1-Score	0,75	0,82	0,75	0,71

Table 11 show EfficientNetB1 consistently shows the highest F1-score values across most periapical lesion types, indicating its robustness in achieving a balance between precision and recall for positive case classification.

MobileNet also demonstrates good performance, especially in Primary Endo with Secondary Perio and Primary Perio with Secondary Endo.

ResNet50v2 performs well in classifying Primary Endodontic Lesions and True Combined Lesions, but it shows slightly lower F1-score

values compared to EfficientNetB1 and MobileNet in other lesion types.

The Shallow model generally has lower F1-score values across all lesion types, indicating its limited capability compared to the other CNN models.

Overall, EfficientNetB1 exhibits the highest average F1-score (0.82), making it the most effective model in diagnosing periapical lesions in this study. MobileNet also performs well with an average F1-score of 0.74. The results suggest that EfficientNetB1 and MobileNet are more suitable for this classification task compared to ResNet50v2 and Shallow models.

Table 11. Comparison F1-Score

Periapical	ResNet50v2	EfficientNetB1	MobileNet	Shallow
Primary Endo with Secondary Perio	0,81	0,84	0,86	0,80
Primary Endodontic Lesion	0,79	0,79	0,7	0,57
Primary Perio with Secondary Endo	0,71	0,86	0,74	0,77
Primary Periodontal Lesion	0,72	0,75	0,67	0,80
True Combined Lesions	0,73	0,87	0,74	0,65
Weight Average F1-Score	0,76	0,82	0,75	0,71

CONCLUSION

Based on the testing and analysis results, it can be concluded that the periapical X-ray classification using the CNN method is capable of classifying X-ray images effectively. The testing process involved data augmentation and the determination of hyperparameters to create various CNN models with different accuracy values in the classification process.

The CNN testing was conducted using four different models to find the best accuracy in the classification. Apart from accuracy, the evaluation of the models was also performed using the confusion matrix method to find the F1-score, which is important due to the imbalanced dataset used, requiring a detailed assessment.

Based on the testing, it was found that the accuracy values using the confusion matrix method for the CNN models (ResNet50v2, EfficientNetB1, MobileNet, and Shallow) are capable of recognizing the periapical X-ray dataset well by classifying the 5 types of X-rays. The highest accuracy result was achieved by the EfficientNetB1 model with an accuracy of 82%, followed by ResNet50v2 with 76%, MobileNet with 75%, and Shallow with 71%.

REFERENCES

[1] R. Ismail Hardianzah, B. Hidayat, F. Teknik Elektro, And U. Telkom Jl Telekomunikasi Terusan Buah Batu Bandung, “Image Processing Of Periapical Radiograph On Pulpitis Detection Using Adaptive Region Growing Approach Method Based On Android,” 2017.

[2] M. Louisa, “Lesi Endoperio 1,” 2015.

[3] B. Indra And S. Huldani, “Dental Radiography and Cellular Immunity: Platelets, Hemoglobin, and Leukocytes”,2019.

[4] C. W. Li *Et Al.*, “Detection Of Dental Apical Lesions Using Cnns On Periapical Radiograph,” *Sensors*, Vol. 21, No. 21, Nov. 2021, Doi: 10.3390/S21217049.

[5] S. M. R And M. Tech Student, “Classification Of Dental Disease Using Cnn,” 2020. [Online]. Available: Http://Ljesc.Org/

[6] University Of Buner. Department Of Electronics & Computer Science And Institute Of Electrical And Electronics Engineers, *1st International Conference On Electrical, Communication And Computer Engineering (Icecce 2019) : 24th - 25th July 2019, Swat, Pakistan*.

[7] A. Thomas, R. N. Firman, And A. Azhari, “Analysis Of Periapical Radiographs Using Imagej Software On Periapical Granuloma In Endodontic Treatment.” *Indonesian Dental Journal*, Vol. 3, No. 2, P. 105, Dec. 2017, Doi: 10.22146/Majkedgiind.10472.

[8] M. Tan And Q. V Le, “Efficientnet: Rethinking Model Scaling For Convolutional Neural Networks”,2019.

[9] Fangyuan Lei, Xun Liu, Jianjian Jiang, Qingyun Dai, Hongyu Liu, Mengying Hu.” Shallow Convolutional Neural Network for Image Recognition”,2019.Doi: 10.17706/ijcee.2019.11.4.192-197

[10] Agung Wahyu Setiawan.” Comparison Of Convolutional Neural Network Architecture In The Classification Of Pneumonia, Covid-19, Lung Opacity, And

Normal Using Thorax X-Ray Image",2022. DOI: 10.25126/jtiik.202296742.

[11] Made Windu Antara Kesiman; Kadek Teguh Dermawan; I Gede Mahendra Darmawiguna. "Balinese Carving Ornaments Classification Using InceptionResnetV2 Architecture",2023. DOI:10.1109/CENIM56801.2022.10037265.

[12] Yuni Naomi Yenusi, Suryasatriya Trihandaru, Adi Setiawan." Comparison of Convolutional Neural Network (CNN) Models in Face Classification of Papuan and Other Ethnicities",2022. https://doi.org/10.23887/jstundiksha.v12i1.46861

[13] Zhafeni Arif, R. Yunendah Nur Fu'adah, Syamsul Rizal, Divo Ilhamdi. "Classification of eye diseases in fundus images using convolutional neural network (CNN) method with efficientnet architecture",2023.DOI: http://dx.doi.org/10.29210/02020344.

[14] Ching-Chen Wang, Ching-Te Chiu, Jheng-Yi Chang. "EfficientNet-eLite: Extremely Lightweight and Efficient CNN Models for Edge Devices by Network Candidate Search",2020. DOI:https://doi.org/10.48550/arXiv.2009.07409

[15] Abdul Rafay a, Waqar Hussain. "EfficientSkinDis: An EfficientNet-based classification model for a large manually curated dataset of 31 skin diseases",2023. DOI: https://doi.org/10.1016/j.bspc.2023.104869.